# PACKET LOSS IN VIDEO TRANSFERS OVER IP NETWORKS

*Fei Xue, Velibor Markovski, and Ljiljana Trajković*

Simon Fraser University
Vancouver, British Columbia, Canada, V5A 1S6
{fxue, vmarkovs, ljilja}@cs.sfu.ca

## ABSTRACT

In this paper, we investigate the behavior of packet loss in Internet Protocol (IP) networks with two transport protocols: User Datagram Protocol (UDP) and Transmission Control Protocol (TCP). We simulate packet loss in congested networks, and we use wavelet analysis to characterize packet loss collected from the trace driven simulation studies. We also analyze the impact of time-scales on the characterization and modeling of loss processes. Our analysis reveals that the packet loss behavior depends on the underlying transport protocol and that the packet loss in UDP transfers exhibits long-range dependence over the coarser time-scales. Furthermore, we show that packet loss patterns preserve the long-range characteristics of the traffic traces generated by the video sources.

## 1. INTRODUCTION

Packet loss, packet delay, and packet delay jitter are important Quality of Service parameters in video transfers. Large values for any of these parameters degrade the quality of the video application. We present here a detailed study of loss patterns that, in addition to the loss probabilities, may help characterize the loss behavior in packet networks.

A typical approach used to collect data for loss analysis is to perform end-to-end measurements using packet probes [3, 4, 10, 15]. Since such measurements of loss in an operating network are often difficult, an alternative approach is to use network simulation tools for collecting loss data. These tools provide flexibility in choosing parameters that influence network performance. We use the *ns-2* network simulator [9] driven by genuine traffic traces to collect packet loss in video transfers. In our previous work [8, 14] we considered the effects of UDP on packet arrival processes and the loss patterns in the network. In this paper, we extend our work and use various simulation scenarios to compare the effects of both UDP and TCP protocols. We also apply wavelet analysis to investigate the packet loss behavior over various time-scales.

We describe simulation scenarios in Section 2, and we introduce long-range dependent processes and wavelet analysis in Section 3. In Section 4 we present simulation results of packet loss and the wavelet analysis of packet loss processes. We discuss the effect of traffic sources and transport protocols on packet loss in Section 5. We conclude with Section 6.

This research is supported by the NSERC Grant 216844-99 and the BC Advanced Systems Institute Fellowship.

## 2. SIMULATION SCENARIOS

We consider a simple network scenario with an arbitrary number of sources *n* generating traffic and feeding a common router buffer *R* connected to a traffic destination *D*, as shown in Fig. 1 (top). All the sources are sending the same traffic trace, starting at random time points within the traffic trace to avoid synchronization. We simulate three scenarios for delivering a video trace to the traffic destination *D*: (1) all traffic sources use UDP transfers, (2) all traffic sources use TCP transfers, and (3) traffic sources use various ratios of UDP and TCP transfers. We use typical packet sizes of 200 bytes for UDP transfers and 552 bytes for TCP transfers. For mixed UDP and TCP transfers, packet size was set to 552 bytes.

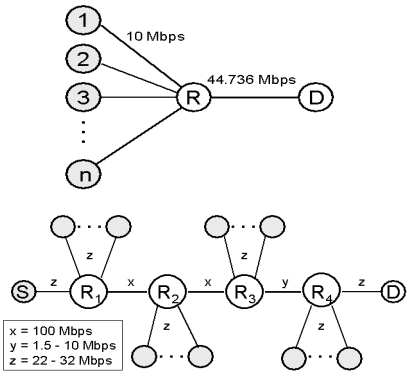


Figure 1: Simple (top) and complex (bottom) network topologies used in simulations of packet loss.

We experiment with various number of traffic sources *n*, in order to cover utilization levels from 50% to 90%. The link speed between the sources and the router *R* is 10 Mbps, and the link speed between the router *R* and the destination *D* is 44.736 Mbps. The router employs a FIFO queuing discipline buffer with a "Drop Tail" queue management policy. By varying the buffer size *B*, we vary the maximum queuing delay from 12.64 to 37.9 msec. These values for the delay are reasonable for video communications, where interactive applications can sustain latencies between 5 and 300 msec [6].

The simulations are trace-driven with a genuine, MPEG-1 encoded, *Star Wars* video trace [11]. The trace consists of more than 170,000 video frames, is coded with 24 frames per second, and is approximately two hours long. Our simulation runs usually last over 20 min.

## 3. LONG-RANGE DEPENDENCE AND WAVELET ANALYSIS

Previous studies have shown that video traffic possesses a complex correlation structure [2] and exhibits long-range dependence (LRD). Long-range dependence has been found in network traffic measured from a wide range of high-speed networks such as Ethernet local area networks, wide area networks, and the Internet [5, 7]. It has also been found that LRD is an inherent feature of VBR video traffic, independent of codec algorithms [2]. Wavelet analysis proved to be a useful tool to analyze the LRD properties of network traffic [1]. Here, we use wavelet analysis in order to understand the behavior of packet loss processes on various time-scales, and to detect the presence of LRD.

### 3.1. Long-range dependence

Let $X(k), k = 0, 1, ...,$ be a *covariance stationary* (sometimes called *wide-sense stationary*) stochastic process with mean *m*, variance $\sigma^2$, and autocorrelation function $r(\lambda), \lambda \geq 0$. $X(k)$ is said to exhibit *long-range dependence* if

$$r(\lambda) \sim c_r \lambda^{-(2-2H)}, \qquad \lambda \to \infty, \tag{1}$$

where $c_r > 0$ and $0.5 < H < 1$. The key element in this description is the Hurst parameter *H* that measures the degree of long-range dependence. For short-range dependent processes $H = 0.5$. Eq. (1) indicates that long-range dependence is characterized by an autocorrelation function that decays hyperbolically as the lag $\lambda$ increases. For example, the genuine *Star Wars* video trace, which is used in our simulation, exhibits LRD with Hurst parameter $H \approx 0.8$ [2].

### 3.2. Wavelets and LRD detection

A wavelet-based Hurst parameter estimator, suggested in [1], is based on a spectrum estimator $\Gamma_x$ designed by finding a time average of $|d_x(j,k)|^2$ at a given scale level $j$:

$$\Gamma_x(2^{-j}\nu_0) = \frac{1}{n_j} \sum_k |d_x(j,k)|^2, \tag{2}$$

where $d_x(j,k)$ are the detail coefficients obtained from the discrete wavelet transform of time series $X(k)$ at scale $2^j$, and $n_j$ is the number of wavelet coefficients at scale level *j*. A linear relationship between $log_2(\Gamma)$ and *j* over a range $[j_1, j_2]$ indicates the presence of an LRD behavior. We can find an estimator $\hat{H}$ for the Hurst parameter $H$ by performing a linear regression of $log_2(\Gamma)$ on scale level $j$ in the range $[j_1, j_2]$:

$$log_2(\Gamma_x(2^{-j}\nu_0)) = (2\hat{H} - 1)j + \hat{c}. \tag{3}$$

We have evaluated the performance of this wavelet-based estimator for a variety of genuine and synthetically generated traffic traces [13]. An example of the wavelet analysis graph for the *Star Wars* trace is shown in Fig. 2.

Rather than focusing on the quantitative aspects of the LRD estimation emphasized in [1], we choose a more qualitative use of the wavelet-based analysis [5]. We use the $log_2(\Gamma)$ vs. $j$ plots to examine the scaling behavior of data. From the plots, we can identify the range of scales with the linear relationship between $log_2(\Gamma)$ and $j$, which indicates the time-scales where LRD is present. These plots also enable us to determine the time-scale break-point beyond which we can accurately detect the LRD. Hence, this technique may be used to detect *both* the presence and the location of LRD.

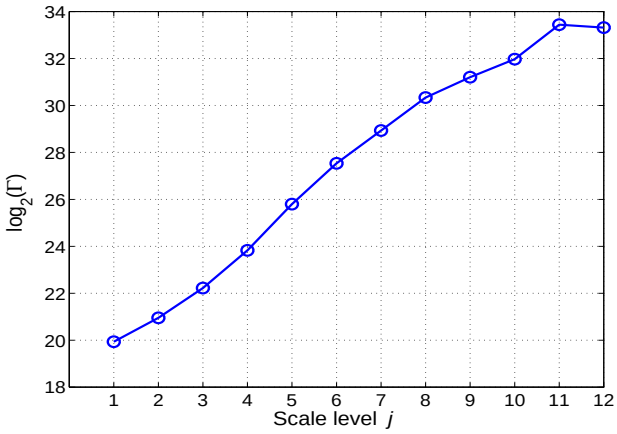


Figure 2: The $log_2(\Gamma)$ vs. *j* plot for *Star Wars* traffic trace.

## 4. CHARACTERIZATION OF PACKET LOSS

We conducted a series of simulation studies in which we varied the number of sources *n* in a network, and the maximum buffer size *B* in the network routers. We recorded lost (dropped) packets and the corresponding instances of loss. Our past analysis of packet loss reported in [8, 14] indicated that packet loss was bursty. We have obtained similar results with a more complex network topology shown in Fig. 1 (bottom), with traffic generated by Web clients and servers, FTP sources, and UDP video sources and destinations.

### 4.1. Packet loss patterns

We present our simulation results using the textured dot strip plot [12] shown in Fig. 3. The plot depicts the loss pattern of a simulation run with $n = 80$ sources, buffer size $B = 512$ packets, and packet size = 200 bytes. Each dot represents the time instance when the loss occurred. The dots are randomly placed along the vertical axis within the height of the plot. In Fig. 3, A is a high congestion band (between 615 and 625 sec), B is a low congestion band (between 836 and 846 sec), and C and D are two bands with no loss (between 826 and 836 sec, and 846 and 854 sec, respectively). Our results show that longer loss episodes have a noticeably larger share of the overall loss during the periods of high congestion (band A), compared to the loss episodes during low congestion (band B).

### 4.2. Scaling behavior of packet loss

In order to study the loss behavior on various time-scales, we consider samples of the loss rate processes obtained from *ns-2* simulations. Each sample represents the number of lost packets during 1 msec intervals. In Fig. 4, we present results of the wavelet analysis for UDP and TCP transfers. We observe that the packet loss behavior varies over different time-scales indicated by the scale

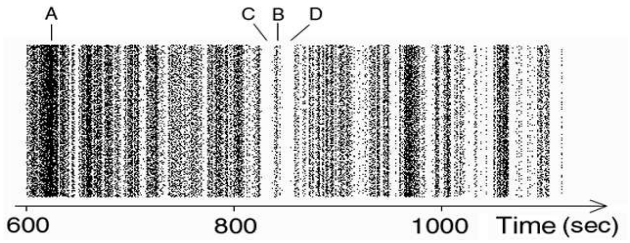


Figure 3: Textured dot strip plot of packet loss instances at the common buffer from a simulation run with $n$ = 80 sources, buffer size $B$ = 512 packets, and packet size = 200 bytes.

level $j$. The graphs also illustrate differences in behavior between UDP and TCP transfers, in particular over the coarser time-scales.

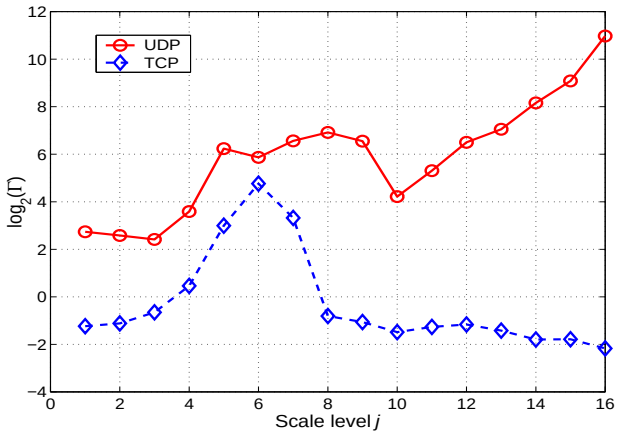


Figure 4: The $log_2(\Gamma)$ vs. $j$ plot of packet loss process for UDP and for TCP transfers: number of sources $n = 160$, buffer size $B = 128$ packets, and packet size $= 552$ bytes.

In the case of UDP transfers shown in Fig. 4, the linear relationship between $log_2(\Gamma)$ and $j$ is evident for the coarser time-scales beyond the break-point $j = 10$. This phenomenon indicates that the time-scale granularity for possible detection of LRD in our example is close to 1,024 ($2^{10}$) msec.

Once the time-scale break-point is observed, we can then create new packet loss rate processes with a numerically more suitable time-scale. For example, we create a loss rate process in which each sample represents the number of loss packets over 1,000 msec, which is close to the estimated time-scale of 1,024 msec where the LRD appears. We then apply the well known Hurst parameter estimators, such as variance-time and R/S analysis [7], to test the presence of LRD and to estimate Hurst parameters. Estimated Hurst parameters for various scenarios range from $0.5$ to $1.0$ [14] and thus indicate that the packet loss process is LRD over time-scales coarser than 1 sec.

For the TCP transfers shown in Fig. 4, the packet loss over the coarser time-scale does not exhibit the LRD behavior, as indicated by the lack of a positive slope in the linear region. This implies that the TCP control mechanisms decrease the burstiness of the packet loss. We are currently investigating the significance of the spectrum peak that appears at time-scales $2^6 = 64$ msec.

## 5. EFFECT OF TRAFFIC SOURCES AND TRANSPORT PROTOCOLS ON PACKET LOSS

In order to understand the effect of the two protocols and the reason for the difference in their behavior, we observe the patterns of aggregate traffic arriving to the common router buffer *R* in Fig. 1.

Wavelet analysis plots of the aggregate traffic arrival processes when traffic sources utilize either UDP transfers or TCP transfers are shown in Fig. 5. Each sample represents the number of packet arrivals during 1 msec intervals. In the case of UDP transfers, the linear relationship between $log_2(\Gamma)$ and $j$ is evident over the coarser time-scales beyond the break-point $j = 10$. Note that the same time-scale break-point ($j = 10$) was observed in the packet loss patterns shown in Fig. 4. For TCP transfers, traffic arrival patterns shown in Fig. 5 are similar to the packet loss patterns shown in Fig. 4. Because the simple "Drop Tail" queue management policy was used in our simulations, this may imply that the "Drop Tail" mechanism preserves the properties of the traffic being transported.

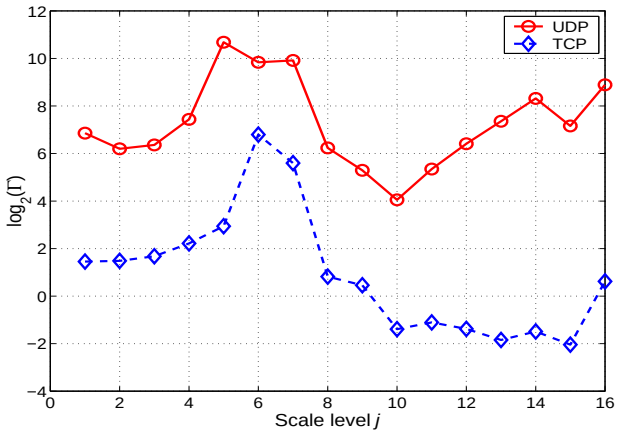


Figure 5: The $log_2(\Gamma)$ vs. $j$ plot of the aggregate traffic arrival process into the router for $n = 160$ sources, buffer size $B = 128$ packets, and packet size $= 552$ bytes.

We have also simulated loss behavior in the case of mixed UDP/TCP transfers in a simple network topology with various contributions of each protocol type. We first compare the average loss probabilities for UDP and TCP sources that share the same link. For the case of 120 UDP sources and 40 TCP sources, the average loss probability for each source is shown in Fig. 6. For each source, the average packet loss probability is calculated as the ratio of the number of dropped packets over the number of generated packets. The loss for the TCP sources is smaller than the loss for the UDP sources, as shown in Fig. 6. The difference may be the consequence of the TCP flow control mechanism.

The wavelet analysis plots of the aggregated packet loss processes are shown in Fig. 7. The loss process is obtained by aggregating the total packet loss in the buffer over every 1 msec interval. The graphs indicate that, as expected, an increase in the ratio of UDP vs. TCP transfers leads to the LRD behavior of loss patterns over the coarser time-scales. In the case of 160 sources

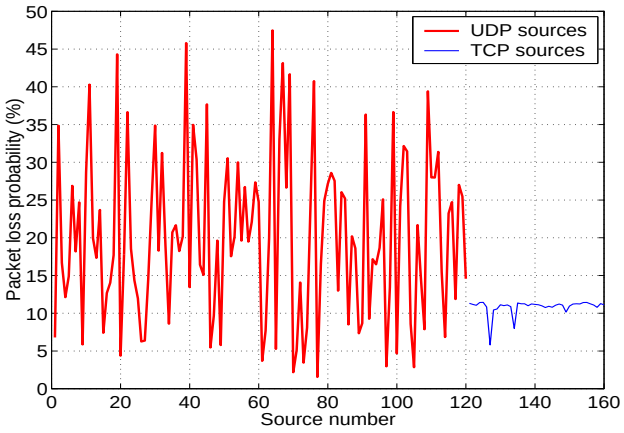


Figure 6: Packet loss probability for each source in mixed UDP/TCP transfer: sources 1 to 120 employ UDP transfers, while sources 121 to 160 employ TCP transfers. Buffer size $B = 128$ packets and packet size $= 552$ bytes.

and a majority of UDP sources (120), the linear region can be observed in Fig. 7. When the number of UDP transfers decreases, the time-scale break-point and the linear behavior disappear.

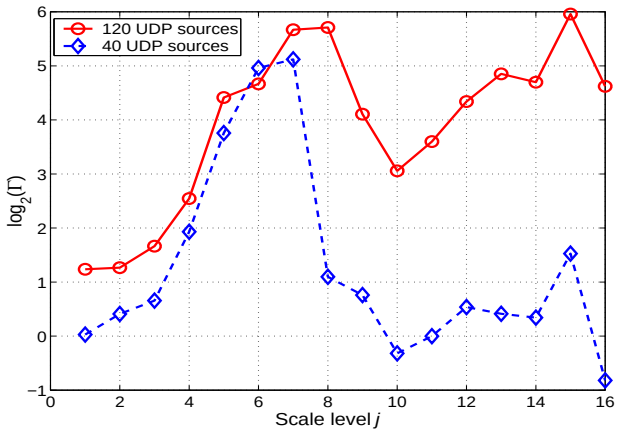


Figure 7: The $log_2(\Gamma)$ vs. $j$ plot of packet loss process for mixed UDP and TCP transfers. Number of sources $n = 160$, buffer size $B = 128$ packets, and packet size $= 552$ bytes.

From simulations of mixed UDP/TCP transfers, we observe the different effect of the UDP and TCP transport protocols on packet loss. UDP transfers tend to cause a loss process that exhibits LRD over the coarser scales, while TCP closed-loop control mechanisms smooth the packet loss. Hence, when designing a packet loss model, the underlying transport protocol should be taken into consideration. This finding may also help explain certain effects in the measured packet loss. For example, the authors in [15] comment that their method might have underestimated the observed correlation time-scales, and that a correlation of the packet loss process over the coarser time-scales is possible. We believe that this effect can be explained by the impact of UDP transfers and need to be considered when modeling packet loss.

We have also examined the linear regions appearing on finer time-scales, both in the case of separate UDP and TCP transfers shown in Fig. 4, and in the case of mixed UDP/TCP transfers shown in Fig. 7. Calculation of the Hurst parameters over those time-scales gives non-physical values $H > 1.0$ that indicate that search for long-range dependence over these time-scales is inconclusive.

## 6. CONCLUDING REMARKS

In this paper, we analyzed packet loss in video transfers over UDP and TCP. We collected packet loss using *ns-2* simulations driven by genuine video traffic traces, and we performed wavelet-based analysis on the collected data over a range of time-scales. The wavelet tool proved helpful in detecting the existence of LRD behavior in loss patterns. In the case of UDP transfers, where LRD behavior was detected on coarser time-scales, we located the break-point level beyond which we calculated Hurst parameters of the packet loss processes. One possible cause for the LRD phenomenon in packet losses under UDP transfers may be that the source traffic itself is LRD. We found that TCP transfers had a smoothing effect on packet loss, which we attributed to the feedback mechanisms of the TCP protocol.

## 7. REFERENCES

[1] P. Abry and D. Veitch, *IEEE Trans. Information Theory*, vol. 44, no. 1, pp. 2–15, 1998.

[2] J. Beran, R. Sherman, M. S. Taqqu, and W. Willinger, *IEEE Trans. Commun.*, vol. 43, no. 2/3/4, pp. 1566–1579, 1995.

[3] J.-C. Bolot, *Proc. ACM SIGCOMM '93*, San Francisco, CA, Sept. 1993, pp. 289–298.

[4] M. S. Borella, D. Swider, S. Uludag, and G. B. Brewster, *Proc. Int. Conf. Parallel Processing*, Minneapolis, MN, Aug. 1998, pp. 3–15.

[5] A. Feldmann, A. C. Gilbert, P. Huang, and W. Willinger, *Proc. ACM SIGCOMM '99*, Aug. 1999, pp. 301–313.

[6] M. Fester, http://www.cisco.com/warp/public/cc/sol/mkt/ent/atm/vidat_wp.htm.

[7] W. Leland, M. Taqqu, W. Willinger, and D. Wilson, *IEEE/ACM Trans. Networking*, vol. 2, pp. 1–15, Feb. 1994.

[8] V. Markovski and Lj. Trajković, *Proc. SPECTS '2K*, July 2000, Vancouver, BC, Canada, pp. 278–285.

[9] ns-2 network simulator: http://www.isi.edu/nsnam/ns.

[10] V. Paxson, *IEEE/ACM Trans. Networking*, vol. 7, no. 3, pp. 277–292, June 1999.

[11] *Star Wars* trace in *ns* format: *http://www.research.att.com/∼breslau/vint/trace.html*.

[12] D. S. Swayne, D. Cook, and A. Buja, *J. Computational and Graphical Statistics*, vol. 7, no. 1, pp. 113–130, Mar. 1998.

[13] F. Xue and Lj. Trajković, *Proc. SPECTS '2K*, July 2000, Vancouver, BC, Canada, pp. 294–298.

[14] F. Xue, V. Markovski, and Lj. Trajković, *Proc. IC '2000*, June 2000, Las Vegas, Nevada, USA, pp. 427–433.

[15] M. Yajnik, S. Moon, J. Kurose, and D. Towsley, *Proc. IEEE INFOCOM '99*, New York, Mar. 1999, pp. 345–352.